Wearable Resonator-Based Respirable Dust Monitor for Underground Coal Mines

Mandana Hajizadehmotlagh, Dorsa Fahimi, Anuj Singhal, *Graduate Student Member, IEEE*, and Igor Paprotny

***Abstract*—Exposure to respirable coal dust and diesel exhaust in underground coal mines can cause detrimental airway diseases such as coal worker's pneumoconiosis (CWP), silicosis, and lung cancer. In this article, we present the design, fabrication, and experimental evaluation of a low-cost wearable respirable dust monitor (WEARDM) that uses a dual-resonator gravimetric sensing approach for real-time measurement of respirable airborne particulate matter (PM) concentrations. The sensor selects for the ISO-respirable dust fraction using a miniature virtual impactor (VI) and removes moisture from the collected dust to ensure accurate mass measurement. WEARDM uses a novel dual-resonator mass sensor (DRMS) that is composed of a quartz crystal microbalance (QCM) and a film bulk acoustic resonator (FBAR). The QCM measures the mass concentration of particles generated from coal mining operations [typically >2.5-μm aerodynamic diameter (AD)], separated using inertial impaction. Thermophoretic precipitation is used to deposit the fine and ultrafine particles, such as those emitted from diesel sources [typically <0.1 μm AD) on FBAR. This allows the WEARDM system to maintain a large dynamic range and uniform collection efficiency (CE) across the entire respirable fraction. The WEARDM system is optimized for a low flow rate of 250 mL/min which results in low power usage and a small form factor and is an order of magnitude smaller and less expensive than currently available devices.**

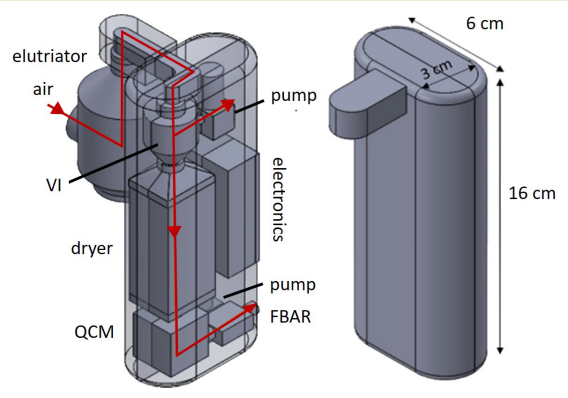

***Index Terms*— Coal dust, diesel exhaust, film bulk acoustic resonator (FBAR), gravimetric mass sensor, particulate matter (PM), quartz crystal microbalance (QCM).**

I. Introduction

AIRBORNE particulate matter (PM) are small solid particles or liquid droplets suspended in the air. These particles are generated by a variety of sources, including coal mining operations and diesel engine usage. PM with a diameter smaller than 100 μm are considered inhalable fractions and can enter deep into the respiratory system. The majority of these particles settle at the beginning of the respiratory tract, but particles with an aerodynamic diameter (AD) smaller than 10 μm (ISO respirable fraction),penetrate deep into the lungs, causing adverse health effects [1], [2]. For instance, lung diseases such as asthma, coal worker's pneumoconiosis (CWP), silicosis, and lung cancer in underground coal miners have been a long-standing problem in the industry. CWP has been the underlying or contributing cause of death for over 75 000 coal miners since the late 1960s and, in recent years, studies have shown an increase in the prevalence of CWP among underground coal workers [3], [4]. In underground coal mines, the main sources of PM are mineral dust with 3–10-μm mass median AD (MMD) and diesel exhaust with 0.15-μm MMD [5]. In 1969, the Federal Coal Mine Health and Safety Act mandated that coal mine dust levels be monitored and kept at or below the permissible exposure limit (PEL). The current Mine Safety and Health Administration PEL is 1.5 mg/m^3 averaged over an 8-h work shift [6].

Optical PM sensors commonly used in low-cost detectors suffer from a number of drawbacks [7]. As a result, the US EPA and NIOSH encourage the use of direct gravimetric

Manuscript received 14 October 2022; revised 9 January 2023; accepted 10 January 2023. Date of publication 16 February 2023; date of current version 31 March 2023. This work was supported by the Center for Disease Control and Prevention (CDC)/National Institute for Occupational Safety and Health (NIOSH), "Miniaturized Wearable Personal Dust Exposure Monitor (WEARDM) for Underground Coal and Silica Mines," under Contract 200-2016-91153. An earlier version of this paper was presented at the 2019 IEEE SENSORS Conference and was published in its Proceedings [DOI: 10.1109/SENSORS43011.2019.8956817]. The associate editor coordinating the review of this article and approving it for publication was Prof. Stefan J. Rupitsch. *(Corresponding author: Igor Paprotny.)*

Mandana Hajizadehmotlagh is with the Department of Physics, University of Illinois at Chicago, Chicago, IL 60607 USA (e-mail: mhajiz2@uic.edu).

Dorsa Fahimi, Anuj Singhal, and Igor Paprotny are with the Department of Electrical Engineering and Computer Science, University of Illinois at Chicago, Chicago, IL 60607 USA (e-mail: dfahim2@uic.edu; asing48@uic.edu; paprotny@uic.edu).

Digital Object Identifier 10.1109/JSEN.2023.3241601

methods for the determination of the PM mass concentrations in underground coal mines [8], [9]. The commercially available respirable dust monitor most commonly used for monitoring coal dust exposure of miners is the Personal Dust Monitor (Model 3700, Thermo Scientific), designed around a tapered element oscillating microbalance (TEOM) technology to record mass concentrations of PM in real-time [10]. The TEOM pulls ambient air through an oscillating filter and heats the air stream to eliminate interference from particle-bound water (PBW). The change in the filter's oscillation frequency due to the captured particles is used to measure the accumulation of mass on the filter over time. The PDM allows miners to monitor their exposure to respirable mine dust in real-time and is recognized by MSHA as a regulatory-grade instrument. However, factors such as considerable weight (2 kg), high cost, a large form factor, and the need for replacing the filter after each shift limits its utility. Also, adsorption and desorption of moisture by the filter can cause positive or negative shifts in the TEOM PM mass measurement, affecting its accuracy [11]. In this article, we introduce an affordable, wearable respirable dust monitor (WEARDM) capable of collecting a uniform distribution of particles across the respirable fraction and providing real-time feedback. WEARDM is able to eliminate the effect of environmental conditions by removing water droplets and moisture from the flow. Due to its flow rate of 250 mL/min, an order of magnitude lower than PDM, it has a greatly reduced form factor and power requirement. The new device builds on prior work in our group on developing air-microfluidic gravimetric PM sensors [12], [13], [14].

II. WEARDM System Overview

A diagram of the airflow through the WEARDM device is shown in Fig. 1. The device contains: (a) an elutriator designed to remove larger particles ($PM_{>10}$) from entering the WEARDM and clogging the channels over time; (b) a fractionator [virtual impactor (VI)] that selects for the respirable fraction from the air stream; (c) a dryer to remove water droplets and moisture from the flow; (d) a dual fraction mass sensor to measure the mass concentration of coal dust and diesel exhaust; (e) micropumps to draw the air stream through the device; and (f) a fan to pull the air through the film bulk acoustic resonator (FBAR) sensor. Off-the-shelf micropumps (Parker Hannifin) are used in the WEARDM system due to their amenability to safety and their small size and weight (14 g, 32 × 22.3 × 13.5 mm^3). Fig. 2 shows the computer-aided design (CAD) model and a fabricated prototype of the WEARDM.

The design parameters and evaluation results of the individual components of the WEARDM are described in detail in Sections III-A–III-D.

III. Modeling and Experimental Evaluation

A. Elutriator

To avoid clogging the air-microfluidic channels with large particles, an inlet elutriator with a 10 μm 50% cut-point is used to stop the large particles from entering the device. The airflow velocity inside the elutriator is defined by the

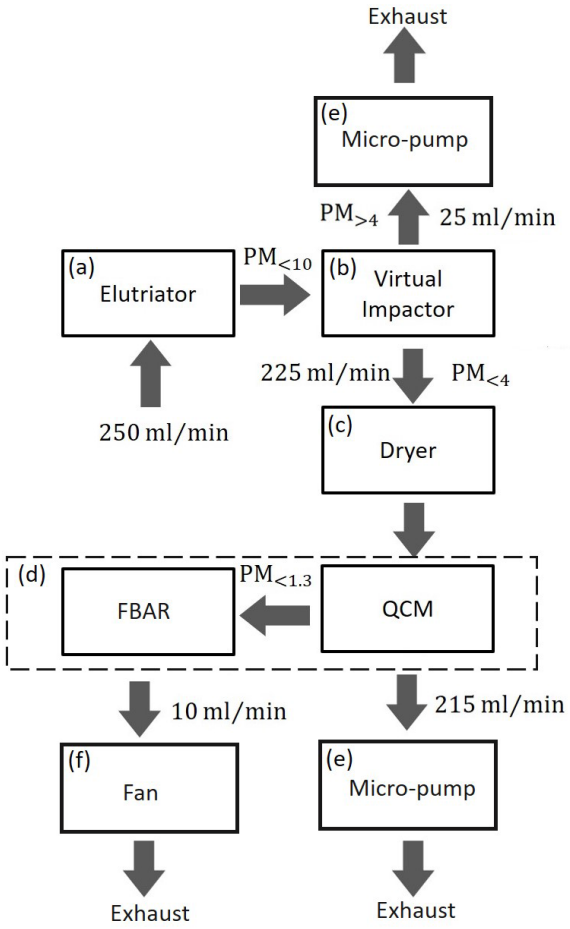

Fig. 1. Flow diagram of the WEARDM system showing the particle fraction and the flow rate selected at each stage. (a) Elutriator, (b) virtual impactor, (c) dryer, (d) dual mass-sensing resonator, (e) micro-pumps, and (f) small fan.

elutriator's inside diameter. Particles with terminal settling velocity (V_{TS}) larger than the flow velocity (V_f) inside the elutriator settle and are removed from the airflow due to gravity, while smaller particles with $V_{TS} < V_f$ are carried upward by airflow and reach the outlet. The designed elutriator has a 42-mm inside diameter to remove particles larger than 10 μm at a 250-mL/min inlet flow rate. V_{TS} is defined as

$$V_{TS} = \frac{\rho_p d^2 g}{18\eta} \tag{1}$$

where ρ_p is the particle density, d is the particle diameter, η is the air viscosity, and g is the downward acceleration due to gravity. A computational fluid dynamics (CFD) modeling software (COMSOL Multiphysics 5.3) was used to optimize the elutriator design and obtain its collection efficiency (CE) across various particle sizes. Fig. 3(a) shows the CAD model for the elutriator and the possible particle trajectories based on their diameters. To evaluate the performance of the elutriator, polydisperse rock dust was aerosolized in the test chamber. The elutriator outlet was connected to a filter and then to a pump (GilAir Plus, Sensidyne) which pulled air at 250 mL/min. Another filter was placed at the bottom of the elutriator to collect the settled particles. After each experiment, the filter surfaces were imaged under a microscope to record

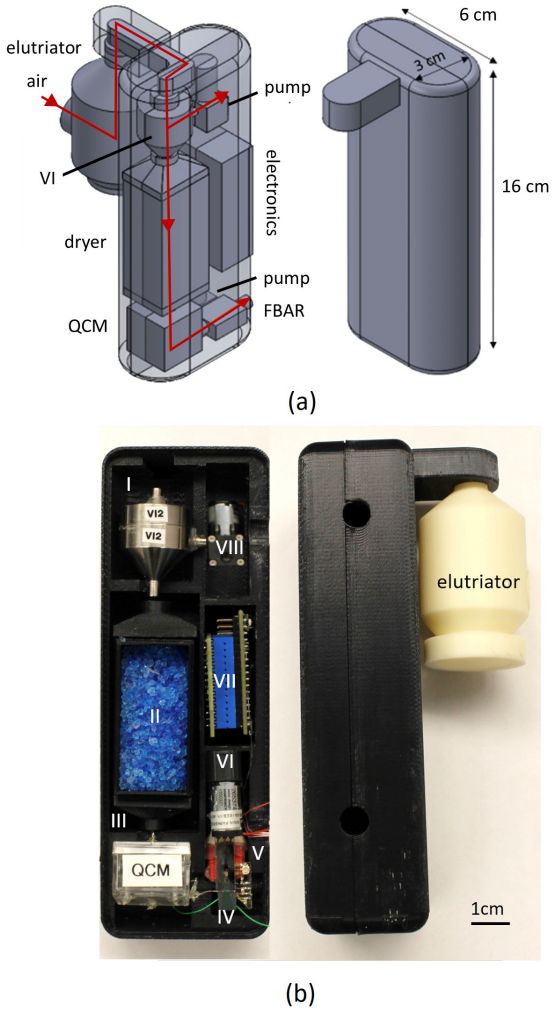

Fig. 2. (a) CAD model showing the flow path inside the WEARDM and the system's dimensions. (b) (Left) Inside view of a fabricated prototype where I) VI, II) dryer filled with desiccants, III) QCM, IV) FBAR, V) fan (mighty mini blower, 12 × 12 × 3 mm, Sunon Corporation) attached to the FBAR's outlet, pulling the air through it, VI) pump drawing the air through the system (T2-05 series, Parker Hannifin Corporation), VII) electronics, and VIII) pump connected to the minor channel. (Right) Side view of the WEARDM with the inlet elutriator.

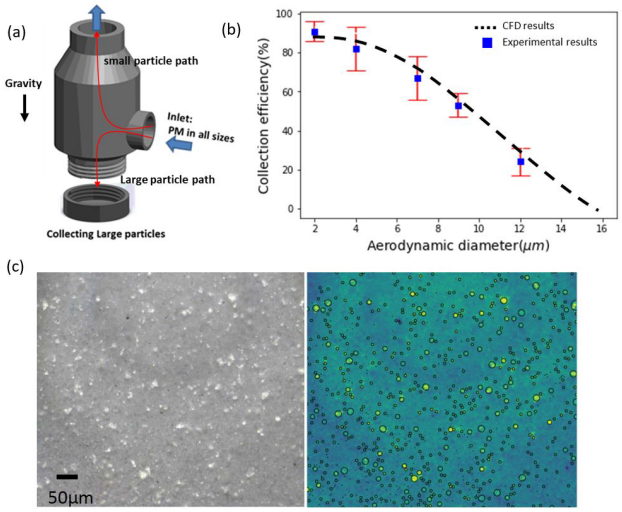

Fig. 3. (a) CAD model of the fabricated elutriator and the possible trajectories of the incoming particles based on their diameter. (b) CFD and experimentally obtained CEs for the elutriator. (c) Section of the collected rock dust particles on a filter after the experiment and the detected particles for CE calculations.

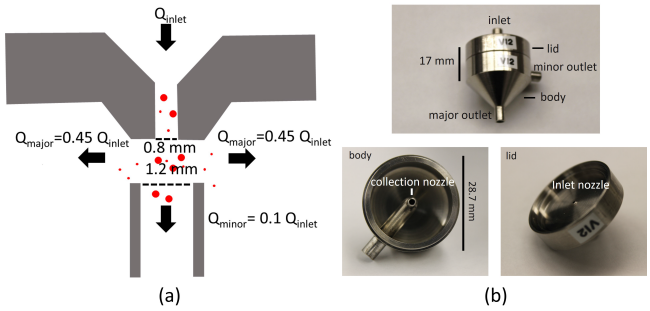

Fig. 4. (a) Schematic showing the design parameters and working principle of the VI. (b) Annotated image of the fabricated VI.

the number of particles collected on each filter. Due to the random shapes of the collected particles, a Python program was used to detect and assign an average diameter to the imaged particles. Fig. 3(c) shows a small section of the outlet filter and the detected particles. To establish the CE, the total area of each filter was imaged and the number of particles for each particle size was counted. The CE for each particle diameter was calculated as

$$\mathrm{CE}(d) = \frac{\text{particle count on outlet filter}}{\text{particle count on outlet and bottom filters}}. \quad (2)$$

The elutriator CE results found by the experimental evaluation and the CFD analysis are shown in Fig. 3(b), demonstrating it can successfully remove large particles. The elutriator (and WEARDM) should be kept vertical; however, because its cut-point is far from the cut-point of the respirable fractionator, a small change (±10°) in orientation will only shift the cut-point slightly and will not affect the respirable fractionator performance.

The elutriator can be replaced with a filter to further decrease the device form factor, although the downside of using filters is that they need to be replaced often to ensure clogging does not affect the inlet flow rate.

B. Virtual Impactor

A VI is commonly used to separate particles into two air streams based on a 50% cut-point AD [15]. In the WEARDM system, the VI is designed to select for the ISO respirable fraction (PM_4) of the collected particles. Particle-laden flow is accelerated in the inlet nozzle, also known as the acceleration jet, and then is divided into two flow streams. To optimize between wall losses and contamination of the minor flow by particles smaller than the cut-point, it is recommended that 10% of the incoming flow (Q_{inlet}) is sent to the minor channel (Q_{minor}), while the other 90% (Q_{major}) is sent to the major channel. Fig. 4(a) shows the working principle of the VI. Particles larger than the VI cut-point cannot follow the sharp 90° turn in the streamlines and are collected in the minor channel, while particles smaller than the cut-point turn 90° and

are collected in the major channel. The 50% cut-point (d_{50}) of a round jet impactor can be determined based on the Stokes number (Stk), flow rate, and injection nozzle width (D_j) as described below [15]

$$d_{50} = \left(\frac{9\eta D_j \mathrm{Stk}_{50}}{\rho_p U C_c}\right)^{1/2} \tag{3}$$

where η is the dynamic viscosity of air, D_j is the diameter of the impactor's jet, ρ_p is the particle density, U is the average air velocity at the nozzle, Stk_{50} is the Stokes number of the jet at the cut-point, and C_c is the Cunningham correction factor. C_c is a function of d_{50} and for particles larger than 0.2 μm can be estimated within a 2% error using the following equation [15]:

$$d_{50} = d_{50}\sqrt{C_c} - 0.078. \tag{4}$$

Fig. 4(b) shows the fabricated VI and the designed parameters for 4-μm 50% cut-point at nominal flow rate. The VI was fabricated using precision CNC machining. To evaluate the performance of the VI, an optogravimetric method was used [16] to experimentally determine the CE. In this method, monodisperse fluorescent polystyrene latex (PSL) microspheres are aerosolized and injected into the VI. The particles are subsequently captured on filters at VI's minor and major flow outlets. A fluorescent microscope is then used to image and count the number of particles on each filter.

To aerosolize the PSL particles (Thermo Scientific), compressed air was passed through a HEPA filter (GelmanLab-12144) and was then directed to the Collison nebulizer to aerosolize PSL particles suspended in deionized (DI) water. Afterward, aerosolized PSLs passed through a diffusion drier where their water content was removed and then were injected into the particle exposure chamber. We used fans to distribute the particles evenly inside the chamber. The VI's major and minor channel air flows were kept at 225 and 25 mL/min, respectively. Airflow at 250 mL/min was also pulled through a reference filter placed next to the VI in the chamber to find the number of particles entering the VI. Using a fluorescent microscope (Zeiss Axio Scope A1), we scanned and imaged the surface of the filters. The experimental setup and collected PSL particles on a portion of a filter are shown in Fig. 5. The CE of the VI for each particle size was determined as

$$\text{Collection efficiency} = \frac{N_{\text{major}}}{N_{\text{inlet}}} \tag{5}$$

where N_{major} is the number of particles collected on the major channel filter and N_{inlet} is the number of particles collected on the reference filter. As shown in Fig. 5(b), the VI follows the ISO sampling criteria for the respirable fraction.

C. Relative Humidity (RH) Preconditioner (Dryer)

A compact Nafion-based dryer was designed to remove water droplets and moisture from the inlet flow before the gravimetric mass sensing step to ensure the measured mass represents dry PM excluding volatile water fraction. Nafion is a polymer with a sulfonic acid group that presents a high affinity for water [17]. In the WEARDM dryer design, the

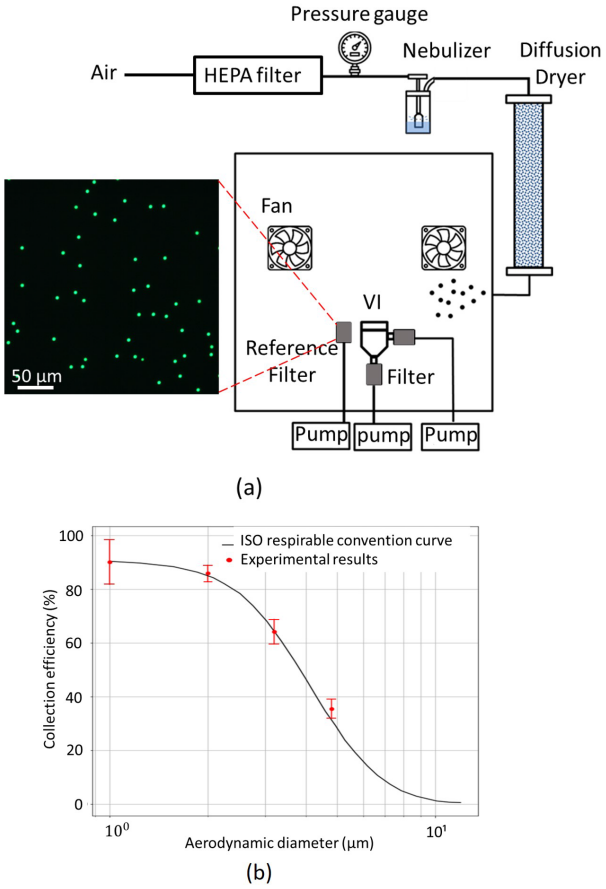

Fig. 5. (a) Test chamber used for exposing the sensors to aerosolized monodisperse PSL particles. (b) Comparison between the ISO convention curve and the experimental CE results of the fabricated VI.

Nafion tubes (Perma Pure) carrying respirable PM fraction were passed through desiccant (silica gel) to generate a water pressure gradient and remove the moisture from the air stream. Due to this gradient, the moisture and water molecules in the flow are absorbed by the Nafion, permeate through it, and finally are absorbed by the desiccants as shown in Fig. 6(b). When saturated, silica gel needs to be replaced or regenerated using in situ integrated heaters (not included here) to ensure the dryer's optimal performance. The water vapor transfer rate in Nafion tubing is a function of the tubing's thickness and surface area, water vapor pressure across the tubing, and flow rate. By dividing the flow among six Nafion tubes, we increased the surface area and decreased the flow rate through Nafion, which resulted in an increase in the water permeation rate through the Nafion tube and enhanced the dryer performance. The efficiency of the WEARDM dryer was experimentally verified by tracking the RH of the flow by placing humidity sensors (Honeywell HumidIcon, HIH8000 Series) with 2.0% RH accuracy, upstream and downstream of the dryer. Fig. 6 shows the fabricated dryer and evaluation results. Nafion tubes are each 6-cm long with 2.2-mm inside diameter. As shown in Fig. 6(c), the dryer successfully maintained the outlet RH below 30% for more than 10 h, when the RH of the inlet flow was around 75%.

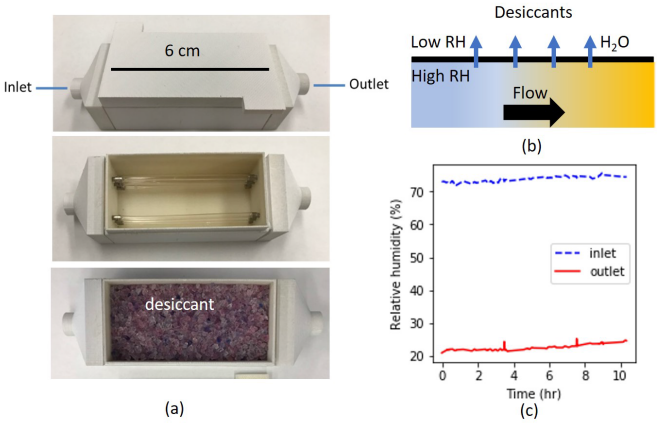

Fig. 6. (a) WEARDM dryer containing six Nafion tubes surrounded by desiccants. (b) Schematic representing the working principle of the Nafion dryer. (c) Data showing the performance of the dryer under high inlet humidity for 10 h.

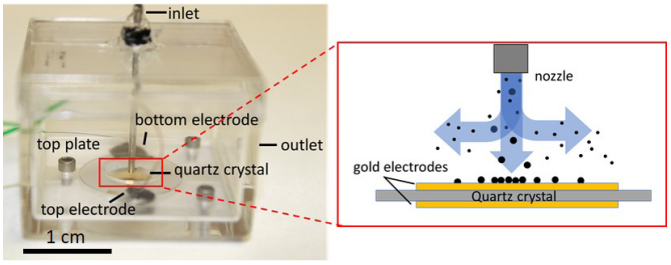

Fig. 7. Fabricated prototype for deposition and mass sensing of the large PM. The prototype includes an inertial impactor with 1.3-μm cut-point and a QCM. The inset schematic shows the working principle of an inertial impactor.

D. Dual-Resonator Mass Sensor (DRMS)

Resonator-based gravimetric mass sensors such as surface acoustic wave (SAW), quartz crystal microbalance (QCM), and FBARs are widely used for real-time direct mass measurements [12], [18]. In resonant-based mass sensors, the addition of mass to the resonating surface causes a decrease in the resonator's resonance frequency. For a small added mass, this change in frequency is linearly proportional to the mass loading. Hence, the mass added to the surface can be calculated using the Sauerbrey equation [19]

$$\Delta m = \frac{\Delta f A \sqrt{\rho_q \mu_q}}{2 f_0^2} \tag{6}$$

where Δm is the mass added to the crystal's surface, f_0 is the resonant frequency of the resonator, Δf is the frequency change, and A, ρ_q, and μ_q are the area, density, and shear modulus of the unloaded piezoelectric crystal, respectively. This model is valid if the amount of mass loading is less than 2% of the resonator mass.

The small size of FBARs (typically 200 $\times$ 200 μm) compared to QCM sensors (typically 14 mm in diameter) makes FBARs a great candidate for lab-on-chip applications where they can be integrated with complementary metal oxide semiconductors (CMOS) in microfluidic devices [12]. Based on the Sauerbrey equation (6), the fundamental resonance frequency has an important role in obtaining higher sensitivity. The resonance frequency of QCM devices is usually in the range of 5–20 MHz, while the resonant frequencies of FBARs can be much higher (hundreds of megahertz to several gigahertz) which results in higher sensitivity and lower detection limits. However, the small size of the FBAR causes it to reach the 2% mass limit quickly compared to QCM sensors when exposed to high PM concentration environments with coarse PM.

To address this issue, the WEARDM system combines two real-time gravimetric resonator-based mass measurement techniques to maintain uniform CE across the entire range of the ISO-respirable PM mass fraction. The first resonant step is designed to collect the bigger portion of the particles (greater than 1.3-μm AD) on the surface of a QCM through inertial impaction [15]. In underground coal mines, this portion generally represents the bulk concentration of the aerosolized mineral dust. The remaining smaller particles (smaller than 1.3-μm AD) are sent into the second resonant stage where a portion of particles are collected on the surface of an FBAR using thermophoretic precipitation. To efficiently capture this smaller fraction, heaters are placed above the FBAR and the thermophoretic force is used to move the particles toward the resonator surface [12]. As a result, the dual resonator can provide real-time mass concentration measurements of mineral dust and ultrafine aerosols such as diesel exhaust.

1) Inertial Impaction on QCM: The working principle of an inertial impactor is similar to that of the VI, but instead of directing the particles larger than the cut-point to the minor channel, particles are collected on an impaction plate surface. QCM is used as the impaction plate and the resulting change in its resonant frequency can be used to record dust concentration in real-time. The fabricated impactor and a schematic showing particle capture using inertial impaction are shown in Fig. 7. The impactor parameters were estimated using (3) and then optimized using CFD modeling to have an approximate cut-point of 1.3 μm. The chosen inlet nozzle diameter and jet-to-impaction plate distance for a 225-mL/min inlet flow rate were 0.52 and 1.0 mm, respectively. The CE found using CFD modeling is shown in Fig. 9(a).

2) Thermophoretic Deposition on FBAR: The design, fabrication steps, and evaluation results of the miniaturized direct-read mass sensor which deposits the particles using thermophoretic precipitation onto a surface of a microfabricated mass-sensitive FBAR was reported previously by Paprotny et al. [12]. The sensor measures 25 $\times$ 21 $\times$ 2 mm in size and has a low flow rate of 10 mL/min. The sensor consists of microfabricated heaters suspended above the mass-sensing FBAR with 250 $\times$ 250 μm^2 surface area inside a 200-μm-high $\times$ 2000-μm-wide channel. The generated temperature gradient across the microfluidic channel creates a thermophoresis force, pushing the particles toward the FBAR surface. For particles with a diameter larger than the mean free path in the air ($\lambda > 0.066$ μm at standard temperature and pressure), the thermophoretic force and velocity can be

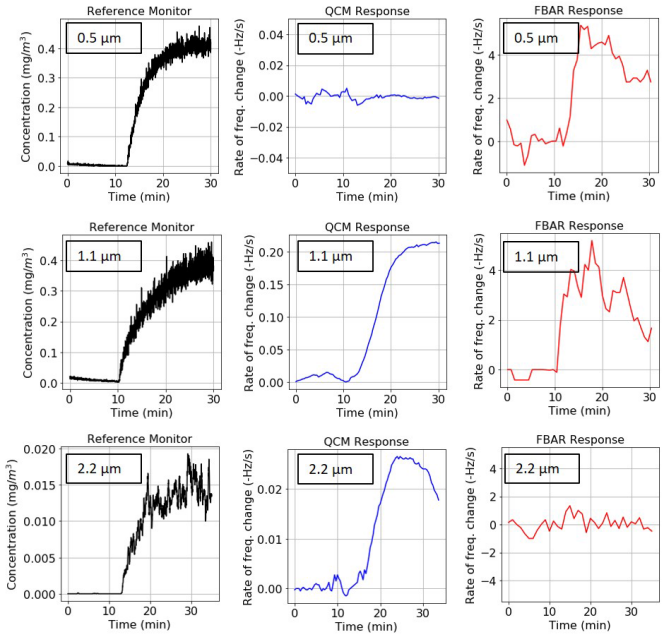

Fig. 8. Representative experiments showing the WEARDM response to 0.5-, 1.1-, and 2.2-μm PSL particles. The slight decrease in the frequency rate of FBAR after deposition of 0.5- and 1.1-μm PSLs is an artifact promoted by the initial step increase of the aerosol concentration in the chamber, as previously observed and described in [12].

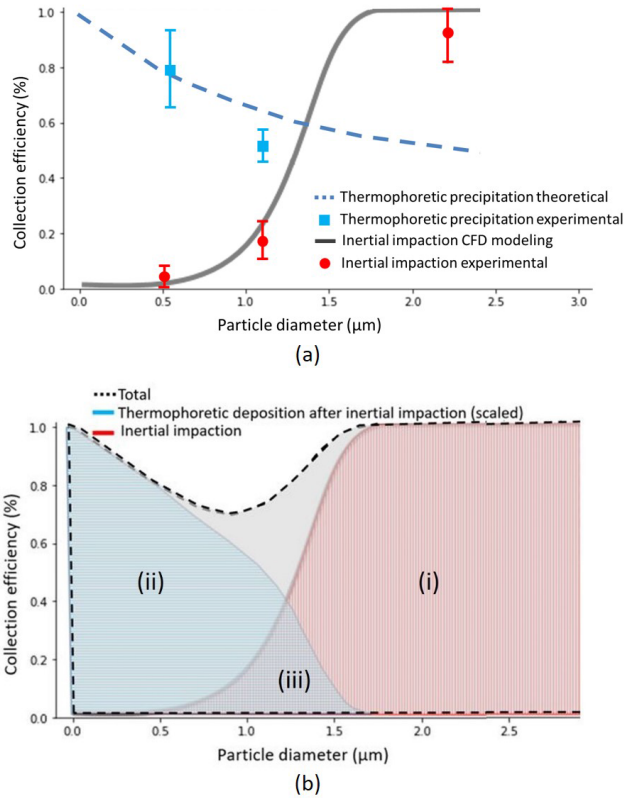

Fig. 9. (a) CEs of the inertial impactor and thermophoretic precipitator obtained using CFD modeling, theoretical analysis, and experimental evaluation. (b) Area denoted by i) shows the CE of the inertial impactor (QCM response) which collects the large particles. The area denoted by ii) shows the CE of the thermophoretic precipitator (FBAR response) when it is placed downstream of the inertial impactor. The thermometric precipitator collects the fine PM. The area denoted by iii) shows the particle sizes that are partially collected by both sensors. The gray highlighted area shows the CE of the WEARDM which is the summation of the two CEs.

found using (7) and (8), respectively [15]:

$$F_{\text{th}} = \frac{-9\pi d_p \eta^2 H \delta T}{2\rho_g T} \tag{7}$$

$$V_{\text{th}} = \frac{-3\eta C_c H \delta T}{2\rho_g T} \tag{8}$$

where δT is the temperature gradient, T is the absolute air temperature, η is the air viscosity, C_c is the Cunningham correction factor, d_p is the particle diameter, and ρ_g is the air density. H is the molecular accommodation coefficient and can be approximately found as

$$H = \left(\frac{1}{1+\frac{6\lambda}{d_p}}\right)\left(\frac{\frac{K_a}{K_p}+4.4\frac{\lambda}{d_p}}{1+2\frac{K_a}{K_p}+8.8\frac{\lambda}{d_p}}\right) \tag{9}$$

where K_a and K_p are the thermal conductivities of air and particles, respectively.

To find the CE of the thermophoretic precipitator, we calculated the thermophoretic velocities of particles with several diameters at a 120 °C temperature gradient. Forward-looking infrared (FLIR) imaging was used to measure the temperature of the heaters, which was between 130 °C and 150 °C (average of 140 °C) and the FBAR was considered at room temperature (20 °C). We used the thermophoretic velocity and the residence time of the particles over the FBAR (calculated based on the 10-mL/min flow rate) to estimate the CE of the thermophoretic precipitator for particles with 0.1–2.5-μm diameters. Fig. 9(a) shows the scaled estimated CE results. It should be noted that the thermophoretic heating also helps to stabilize the thermal noise of the FBAR, which has been temperature compensated for zero slopes at around 20 °C. Additional active-controlled heating, or a differential resonator configuration can be used to further reduce the thermal noise.

3) Dual-Resonator Evaluation: To evaluate the performance of the inertial impactor, monodisperse PSL particles were aerosolized inside the test chamber [see Fig. 5(a)]. The particle-laden flow was pulled through the QCM at 225 mL/min. The AT-cut quartz crystal with gold electrodes and the QCM driver used in these prototypes were purchased from OpenQCM [20]. As shown in Fig. 1, the QCM outlet was connected to the FBAR sensor inlet. OpenQCM software on a connected computer was used to measure and record the frequency response of the QCM during the experiments. A peristaltic pump (Fisherbrand) was used to draw the particle-laden flow at a low flow rate of 10 mL/min through the microfluidic channel with heaters and FBARs. As particles collected on the FBAR, a CMOS circuit wirebonded to the FBAR was driving the FBAR at its resonant frequency which was recorded using an off-board spectrum analyzer (Keysight N9243C). We performed the experiment for 2.2-, 1.1-, and 0.5-μm PSL particles with the respective resonator responses shown in Fig. 8. For 2.2-μm aerosolized PSL particles, the inertial impactor CE was considered 100% when the QCM

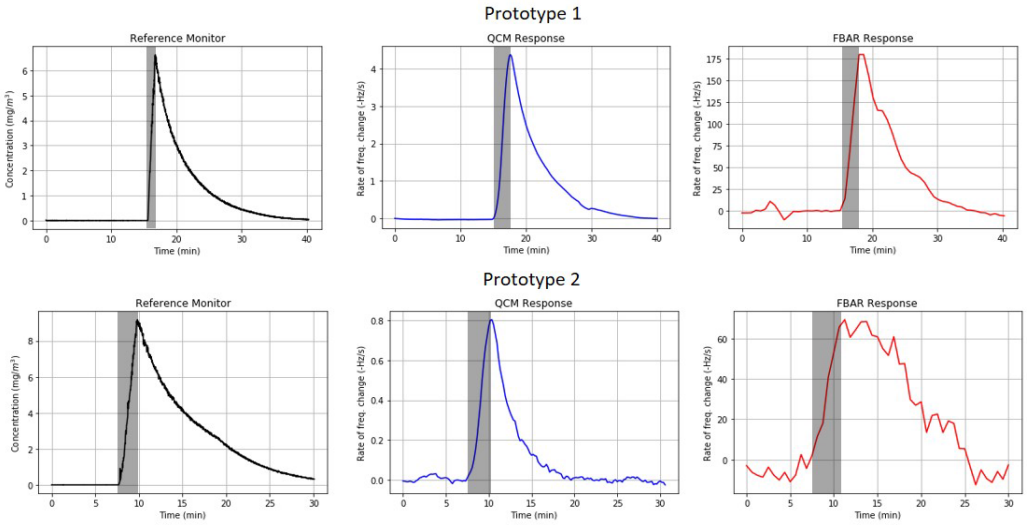

Fig. 10. Representative experiments showing the response of two WEARDM prototypes to polydisperse incense generated PM. The reference monitor shows the PM concentration in the chamber during the experiment. The gray shaded area in the graphs shows the time when the burning incense was introduced to the chamber. The QCM and the FBAR responses are shown in the rate of frequency change over time which is proportional to the mass concentration in the chamber.

showed a negative change in the resonance frequency while no frequency shift was recorded by the FBAR, implying that all particles are collected on the impaction plate. We used the linear relation between the frequency change and the added mass [see (6)] to find the CE for 1.1 and 0.5 μm based on the CE at 2.2 μm for 1-mg/m^3 mass concentration in the test chamber. In the case of the 0.5-μm aerosolized PSL particles, the QCM did not show a significant response and maintained almost the same resonance frequency while the PM senor showed frequency shift due to the mass loading.

To calculate the CE of the thermophoretic precipitator, the FBAR frequency shift for 1- and 0.5-μm particle sizes at 1 mg/m^3 particle mass concentration was measured. We considered the average CE at 0.5 μm to match the theoretically approximated value and found the CE at 1 μm based on that. The evaluation result is shown in Fig. 9(a).

IV. Overall System Evaluation

The CE across the respirable fraction can be found by adding the CE values resulting from the QCM and the FBAR measurements. In Fig. 9(b), the area denoted by i) (vertically striped area) shows the CE due to the inertial impaction on the QCM surface. The impactor cut-point is 1.3 μm and all particles larger than 2 μm are collected in this step. The area denoted by ii) (horizontally striped area) shows the scaled CE due to thermophoretic precipitation downstream the inertial impactor. The overlap between the two graphs is denoted by iii) (crosshatched area) and shows the particle sizes that are partially collected by both sensors. The addition of the two CEs results in the gray highlighted area that is the measured CE of the WEARDM sensor for the respirable fraction. The dual mass sensor resonator can maintain an approximately uniform CE across the bimodal (respirable and ultrafine) particle distribution, collecting both large and ultrafine PM. The CE drops around 1-μm particle diameter which results in lower sensitivity at this particle diameter range but because the MMD of diesel exhaust is approximately 0.15 μm and the MMD of coal dust is between 3 and 10 μm, this low sensitivity would not considerably affect the mass measurement in underground coal mines.

The performance of the complete WEARDM system was evaluated by exposing the device to aerosolized PSL particles as well as polydisperse particles generated from burning incense. The results of exposing the WEARDM to 0.5-, 1.1-, and 2.2-μm particles are shown in Fig. 8. Each experiment included a 10-min stabilization period. The graphs show the mass concentration read by the reference monitor and the rate of frequency change over time for the QCM and FBAR during each experiment. Mass loading per unit time ($-df/dt$) of the resonators is proportional to the particle mass concentration in the test chamber during the experiment. As expected, for particle size below the impactor cut-point (0.5 μm), the QCM did not show a significant response while the FBAR showed particle loading. For 1.1-μm particles, both resonators represented frequency shift showing that particles are collected by both resonators. Particles larger than the cut-point (2.2 μm) were only captured by the QCM.

To expose the WEARDM to polydisperse particles, after stabilization, an approximately 1-cm incense stick was lit and placed into the test chamber. The PM concentration increased until the stick burned out completely and then the concentration declined as the particles settled. Fig. 10 shows a representative response of the QCM and FBAR and the mass concentration measured by the reference monitor during the experiment for two prototypes. The gray column denotes the introduction of the incense-generated aerosol into the chamber.

V. Conclusion

CWP and lung cancer in underground coal miners is a long-standing problem. In this work, we presented the design and fabrication of a low-cost WEARDM and showed the results from the experimental evaluation of the individual

components as well as the integrated system when exposed to monodisperse and polydisperse particles. We showed that the device successfully selects the respirable fraction of the particles, removes moisture, and uses a dual-resonator for continuous mass measurement of coal dust and diesel exhaust. Our experiments confirmed that the WEARDM can maintain an approximately uniform CE across the bulk of the respirable fraction. The WEARDM system works at a low flow rate of 250 mL/min, which results in low power usage (estimated at 50–100 mW) and a small form factor compared to similar commercially available devices. The QCM and FBAR components are expected to be consumable, and in a commercial device will be placed as cartridges that can be replaced when approaching the saturation threshold. The results in Fig. 10 show good repeatability of both resonators for two separate runs of two separate WEARDM prototypes. A follow-up longevity study should be conducted to determine the long-term performance parameters and stability of the WEARDM devices in a representative underground mine environment.

Acknowledgment

The findings and conclusions in this manuscript are those of the authors and do not necessarily represent the views of the National Institute for Occupational Safety and Health (NIOSH). Mention of company names or products does not constitute an endorsement by NIOSH.

References

[1] J. O. Anderson, J. G. Thundiyil, and A. Stolbach, "Clearing the air: A review of the effects of particulate matter air pollution on human health," *J. Med. Toxicol.*, vol. 8, no. 2, pp. 166–175, Jun. 2012.

[2] N. Englert, "Fine particles and human health—A review of epidemiological studies," *Toxicol. Lett.*, vol. 149, nos. 1–3, pp. 235–242, Apr. 2004.

[3] D. J. Blackley, C. N. Halldin, and A. S. Laney, "Continued increase in prevalence of coal workers' pneumoconiosis in the United States, 1970–2017," *Amer. J. Public Health*, vol. 108, no. 9, pp. 1220–1222, Sep. 2018.

[4] D. J. Blackley, C. N. Halldin, and A. S. Laney, "Continued increase in lung transplantation for coal workers' pneumoconiosis in the United States," *Amer. J. Ind. Med.*, vol. 61, no. 7, pp. 621–624, Jul. 2018.

[5] K. L. Rubow, B. K. Cantrell, and V. A. Marple, "Measurement of coal dust and diesel exhaust aerosols in underground mines," *Proc. 7th Int. Pneumoconioses Conf.* Pittsburgh, PA, USA: U.S. Department of Health and Human Services, Aug. 1988.

[6] B. C. Doney et al., "Respirable coal mine dust in underground mines, United States, 1982–2017," *Amer. J. Ind. Med.*, vol. 62, no. 6, pp. 478–485, Jun. 2019.

[7] Y. Wang, J. Li, H. Jing, Q. Zhang, J. Jiang, and P. Biswas, "Laboratory evaluation and calibration of three low-cost particle sensors for particulate matter measurement," *Aerosol. Sci. Technol.*, vol. 49, no. 11, pp. 1063–1077, 2015.

[8] *Health. Division of Physical Sciences. NIOSH, Manual of Analytical Methods*, US Department of Health and Human Services, Public Health Service, Centers, Washington, DC, USA, 1994.

[9] *United States. Environmental Protection Agency. Office of Air Quality Planning and Standards. Review of the National Ambient Air Quality Standards for Particulate Matter: Policy Assessment of Scientific and Technical Information*, DIANE Publishing, Collingdale, PA, USA, 1996.

[10] H. Patashnick and E. G. Rupprecht, "Continuous PM-10 measurements using the tapered element oscillating microbalance," *J. Air Waste Manage. Assoc.*, vol. 41, no. 8, pp. 1079–1083, 1991.

[11] A. Charron, "Quantitative interpretation of divergence between PM_{10} and $PM_{2.5}$ mass measurement by TEOM and gravimetric (Partisol) instruments," *Atmos. Environ.*, vol. 38, no. 3, pp. 415–423, Jan. 2004.

[12] I. Paprotny, F. Doering, P. A. Solomon, R. M. White, and L. A. Gundel, "Microfabricated air-microfluidic sensor for personal monitoring of airborne particulate matter: Design, fabrication, and experimental results," *Sens. Actuators A, Phys.*, vol. 201, pp. 506–516, Oct. 2013.

[13] D. Fahimi, O. Mahdavipour, J. Sabino, R. M. White, and I. Paprotny, "Vertically-stacked MEMS $PM_{2.5}$ sensor for wearable applications," *Sens. Actuators A, Phys.*, vol. 299, Nov. 2019, Art. no. 111569.

[14] M. Hajizadehmotlagh, A. Singhal, and I. Paprotny, "Enhanced capture of aerosol particles on resonator-based PM mass sensors using staggered arrays of micro-pillars," *J. Microelectromech. Syst.*, vol. 29, no. 5, pp. 1044–1048, Oct. 2020.

[15] W. C. Hinds and Y. Zhu, *Aerosol Technology: Properties, Behavior, and Measurement of Airborne Particles*. Hoboken, NJ, USA: Wiley, 2022.

[16] O. Mahdavipour, D. Fahimi, and I. Paprotny, "Focusing of airborne particles using groove-induced envelope (GRIP) flow air-microfluidic concentrator," *J. Microelectromech. Syst.*, vol. 28, no. 3, pp. 453–459, Jun. 2019.

[17] P. W. Majsztrik, M. B. Satterfield, A. B. Bocarsly, and J. B. Benziger, "Water sorption, desorption and transport in Nafion membranes," *J. Membrane Sci.*, vol. 301, nos. 1–2, pp. 93–106, Sep. 2007.

[18] W. D. Bowers, R. L. Chuan, and T. M. Duong, "A 200 MHz surface acoustic wave resonator mass microbalance," *Rev. Sci. Instrum.*, vol. 62, no. 6, pp. 1624–1629, Jun. 1991.

[19] G. Sauerbrey, "The use of quarts oscillators for weighing thin layers and for microweighing," *Z. Phys.*, vol. 155, pp. 206–222, Jan. 1959.

[20] *Open QCM*. Accessed: Oct. 2, 2022. [Online]. Available: https://openqcm.com

Mandana Hajizadehmotlagh received the B.S. degree in solid-state physics from the K. N. Toosi University of Technology, Tehran, Iran, in 2011, the M.S. degree in nanotechnology from the University of Tehran, Tehran, in 2014, and the Ph.D. degree in physics from the University of Illinois at Chicago (UIC), Chicago, IL, USA, in 2019.

As a Research Assistant at the Micromechatronic Systems Laboratory, UIC, her research interests include the design, fabrication, and analysis of particulate matter sensors with a focus on air microfluidics and resonators.

Dorsa Fahimi received the B.Sc. degree in electrical engineering from the University of Tehran, Tehran, Iran, in 2013. She is currently pursuing the Ph.D. degree in electrical and computer engineering with the University of Illinois at Chicago, Chicago, IL, USA.

Her research interests include MEMS, air-microfluidics, and air quality sensors.

Anuj Singhal (Graduate Student Member, IEEE) received the Bachelor of Technology degree in electronics and communication engineering from Kurukshetra University, Thanesar, India, in 2017. He is pursuing the Ph.D. degree with the University of Illinois at Chicago (UIC), Chicago, IL, USA.

He joined the Micromechatronics System Laboratory, UIC, in 2018. He works as a Research Assistant with the Nanotechnology Core Facility (NCF), UIC. His research interests include nanofabrication, microoptics, and air-microfluidics.

Igor Paprotny received the Ph.D. degree in computer science from Dartmouth College, Hanover, NH, USA, in 2008.

He is currently an Associate Professor with the Department of Electrical and Computer Engineering, University of Illinois at Chicago, Chicago, IL, USA. He has authored five book chapters, more than 50 papers in journals and conferences, and holds four patents. His research interests include microrobotics, energy systems sensing, and air-microfluidics.